

Original Paper

Tumor-Secreted Exosomal miR-222 Promotes Tumor Progression via Regulating P27 Expression and Re-Localization in Pancreatic Cancer

Zhonghu Li^a Yang Tao^b Xiaoya Wang^c Peng Jiang^d Jie Li^d Minjie Peng^e
Xi Zhang^d Kai Chen^d Hui Liu^e Ping Zhen^d Jin Zhu^d Xiangde Liu^d Xiaowu Li^{d,e}

^aHepatobiliary Surgery Institute, Southwest Hospital, Army Medical University, Current address: Department of General Surgery, General Hospital of Wuhan, People's Liberation Army, Wuhan,

^bChongqing Key Laboratory of Translational Research for Cancer Metastasis and Individualized Treatment, Chongqing University Cancer Hospital & Chongqing Cancer Institute & Chongqing Cancer Hospital, Chongqing, ^cDepartment of Neurosurgery, the Second Affiliated Hospital of North Sichuan Medical College, Nanchong, ^dHepatobiliary Surgery Institute, Southwest Hospital, Army Medical University, Chongqing, ^eHepatobiliary Surgery & Carson International Cancer Shenzhen University General Hospital & Shenzhen University Clinical Medical Academy Center, Shenzhen University, Shenzhen, China

Key Words

Pancreatic cancer • Exosome • miRNA • P27 • Tumor invasion • Tumor prognosis

Abstract

Background/Aims: MicroRNAs (miRNAs) or exosomes have recently been shown to play vital regulatory or communication roles in cancer biology. However, the roles and mechanisms of exosomal miRNAs in pancreatic ductal adenocarcinoma (PDAC) remain unknown. We aimed to investigate the detailed roles and mechanisms of tumor-generated exosomal miRNAs in progression of PDAC. **Methods:** miR-222 was identified by miRNA microarray studies in exosomes of PDAC cells, and further analyzed in plasma exosomes of PDAC patients. The regulatory mechanisms of miR-222 were explored by qRT-PCR, WB, dual-luciferase assays and immunofluorescence or confocal analysis. Other biological assays include transwell, xenograft models and so on. **Results:** miR-222 is significantly high in tumor exosomes or highly invasive PDAC cells. miR-222 could directly regulate p27 to promote cell invasion and proliferation. miR-222 could also activate AKT by inhibiting PPP2R2A expression, thus inducing p27 phosphorylation and cytoplasmic p27 expression to promote cell survival, invasion and metastasis. Expressions of miR-222 and p27 were significantly inversely correlated, and cytoplasmic p27, instead of nuclear p27, was associated with tumor malignancy. miR-222 could be transmitted between PDAC cells via exosome communication, and the exosomal

Z. Li and Y. Tao contributed equally to this work.

Xiangde Liu, MD-PhD
and Xiaowu Li, MD-PhD

Hepatobiliary Surgery Institute, Southwest Hospital, Army Medical University
No. 30 Gaotanyan Street, Shapingba District, Chongqing 400038 (China)
Tel. 86-23-68765805, Fax 86-23-65317637, E-Mail lixw1966@163.com

miR-222 communication is functional. Plasma exosomal miR-222 in PDAC patients was high and significantly correlated to tumor size and TNM stage, and was an independent risk factor for PDAC patient survival. **Conclusion:** Tumor-generated exosomes could promote invasion and proliferation of neighboring tumor cells via miR-222 transmission, the plasma exosomal miR-222 plays important roles and may be a useful prognostic maker in PDAC.

© 2018 The Author(s)
Published by S. Karger AG, Basel

Introduction

With a 5-year survival rate of approximately 5%, pancreatic ductal adenocarcinoma (PDAC) is the deadliest of all solid malignancies [1, 2]. Surgical resection remains the only potentially curative therapy, but most PDAC patients are diagnosed at advanced stages and miss their chance for operation [3, 4]. This disappointing outcome is partly due to the uncontrolled rapid tumor growth and invasion of PDAC. Many studies have revealed that tumor growth and invasion are complicated processes that involve many oncogenes or pathways [5]. p27 Kip1(p27), also called cyclin-dependent kinase inhibitor B, is one of the most important oncogenes related to tumor cell cycle regulation and tumor invasion [6, 7]; the PI3K/AKT signaling pathway also participates in many physiological processes, including cell proliferation and apoptosis inhibition [8, 9]. Detecting the pathological and molecular mechanisms of PDAC may facilitate the discovery of new therapeutic targets or diagnostic biomarkers in clinical practice.

MicroRNAs (miRNAs) are a class of small noncoding RNAs that negatively regulate gene expression at the post-translational level [10]. By binding to the 3'UTR of the target gene, miRNAs mediate translational repression primarily via mRNA degradation [11, 12]. To date, a large number of tumor-related miRNAs have been identified to play key roles in many biological processes, including cell proliferation, invasion, and metabolism [13-15]. However, the majority of identified miRNAs are tumor suppressor genes; although several studies have reported serum miRNA correlations with different tumors, such studies of PDAC are rare, and the origins of the serum miRNAs remain unidentified [16]. Thus, the investigation of serum tumor-promoting miRNAs in PDAC is urgently needed.

Exosomes are small membrane vesicles (diameters ranging from 40-100 nm) that are saucer-like flattened spheres released from different cells [17]. Exosomes were first identified in mammalian reticulocytes, but their presence has been confirmed in different tumor cells; they can transfer a wide variety of biological components, including proteins, miRNAs, mRNAs, lncRNA and circular RNAs, to other recipient cells via cellular communication [18, 19]. Recently, more and more studies have shown that tumor exosomes play key roles in cell communication, the immune system and tumor invasion. Thus, biomarkers in exosomes may be suitable for diagnostic use in clinical practice [20, 21]. So far, several studies have shown that tumor-related miRNAs exist in exosomes and play important roles in angiogenesis, tumor invasion and metastasis [22-24]. However, the origin of miRNAs in exosomes remains unclear, and studies of tumor-related miRNAs in exosomes in PDAC are unknown.

In this study, we identified a tumor-promoting miRNA (miR-222) in tumor exosomes by microarray analysis; its functions and detailed molecular mechanisms were also determined. We further confirmed the transfer of miR-222 between tumor cells by exosomes, and the expression of miR-222 in plasma exosomes was also analyzed in clinical PDAC samples. Ultimately, we further proved the tumor released miR-222 in blood exosomes *in vivo* conditions and put forward a hypothesis about how tumor released miR-222 functions in pancreatic cancer.

Materials and Methods

Cell culture and transfection

The Pancreatic ductal adenocarcinoma (PDAC) cell lines AsPC-1, BxPC-3, Capan-1, Hs 766T, PANC-1 and SW 1990 were purchased from ATCC, HEK 293 and normal pancreatic cell HPDE were also purchased from ATCC. Hs 766T-L1, Hs 766T-L2 and Hs 766T-L3 are the first, second and third generation primary cells from liver metastatic tissue of Hs 766T as described in our last paper, respectively. Daughter cell lines of Hs 766T were further authenticated by STR profiling. PDAC cells were cultured in RPMI-1640 medium (Gibco, USA) and HEK-293, HPDE were cultured in DMEM supplemented with 10% fetal bovine serum (FBS) (Gibco, USA) at 37°C in a humidified atmosphere containing 5% CO₂.

Cell transfections were carried out as described previously. Briefly, for lentivirus transduction, 10⁵ PDAC cells were incubated in a 6-well plate with 2 ml of medium containing 100 µl (10⁷ U) of lentivirus particles and 5 µg/ml polybrene for 24 h. Plasmid and siRNA transfections were performed using Lipofectamine 3000 (Invitrogen, USA) according to the manufacturer's instructions. miRNA mimics or scramble control RNAs (RiboBio, China) were transfected into cells at a final concentration of 100 nM using a riboFECTTM CP Kit (RiboBio, China) according to the manufacturer's instructions, oligo sequence of cy5-miR-222: S: AGCUACAUCUGGCCUACUGGGU, A: CCAGUAGCCAGAUGUAGCUUU.

Exosome experiments

All exosomes assays contained in this study were similar with our last paper. Briefly, PDAC cells were cultured with conditioned medium with 10% d-FBS, and 10 ml culture medium was used for exosomes extraction by Total Exosome Isolation Kit (Thermo, USA). To label exosomes, 2.5 µg/ml Dil was added before the mixture were centrifuged for 1 h. Plasma exosomes extraction was carried out as previous discussed, briefly, 2 ml of fresh plasma was collected from each patient and the exosomes were extracted using ExoQuick™ Exosome Precipitation Solution (SBI, USA).

For exosomes quantification, the FLUOROCET Ultrasensitive Exosome Quantitation Assay Kit (SBI, USA) was used to ensure the same number of exosomes was used in each experiment. As discussed before, 5×10⁸ exosomes were used for exosomal RNA extraction, 1×10⁸ exosomes were used for exosomes-stimulation experiment *in vitro*. The size and morphology were further confirmed by transmission electron microscopy (TEM).

Microarray analysis

Exosomes of Hs 766T and Hs 766T-L2 cells were purified and total RNAs were extracted using TRIzol LS (Thermo, USA) according to the manufacturer's instructions, then RNAs were treated with RNase R to remove other non-circular RNAs. RNA expression profiling was performed using Arraystar Human miRCURYTM LNA Array (Arraystar, USA). Briefly, After quality control, the miRCURY™ Hy3™/Hy5™ Power labeling kit (Exiqon, Vedbaek, Denmark) was used according to the manufacturer's guideline for miRNA labelling. After stopping the labeling procedure, the Hy3™-labeled samples were hybridized on the miRCURYTM LNA Array (v.18.0) (Exiqon) according to array manual. Then the slides were scanned using the Axon GenePix 4000B microarray scanner (Axon Instruments, Foster City, CA).

Cell migration and invasion assay

Cell migration was examined by a wound-healing assay according to previously described. Briefly, PDAC cells were cultured regularly until reaching confluence and the medium was replaced with serum-free 1640 medium, wounds were made with a 10 µl-pipette tip and photos were captured by phase-contrast microscope. Cell invasion ability was evaluated by a transwell assay as described previously. Briefly, 5×10⁵ PDAC cells in 300 µl of serum-free medium were cultured in a chamber containing an 8 µm polycarbonate filter (Millipore, USA) coated with 30 µl of Matrigel (BD, USA), After incubating for 36 h, cells remaining on the upper membrane were removed with a cotton swab and cells that had penetrated the membrane were fixed with 4% formaldehyde and then stained with 0.5% crystal violet for 20 min. All the statistical results were obtained from three independent experiments averaged from five randomly selected image fields.

Plasmids

Plasmids used in this study include miR-222 overexpression, miR-222 shRNA, pGL3 p27 and pGL3 mut-p27 luciferase plasmids. All of the plasmids listed above were designed and provided by Sangon. Ltd. China and were confirmed by DNA sequencing with sequencing reports provided.

Immunofluorescence

Immunofluorescence assays were taken as previously described. Briefly, PDAC cells were seeded and cultured on cell slides and then transfected with miRNA or incubated with exosomes, then cells were fixed, permeabilized, blocked by incubating with 1% bovine serum albumin (Sigma, USA). The cells were then incubated with primary antibodies specific for anti-p27 (1:800, #3686, CST, USA) overnight at 4°C. The cells were then incubated with a goat anti-rabbit IgG (fluorescein labeled, 1:500, PIERCE, USA) secondary antibody for 1 h at 37°C. The slides were mounted with Mounting Medium for Fluorescence with DAPI (Vector Laboratories, USA) and imaged with a fluorescence microscope.

5-Ethynyl-2'-deoxyuridine (EdU) incorporation assay

The EdU assay was performed with a keyFluor488 Click-iT EdU detection kit (KGA331-100, KeyGene, Nanjing, China) according to the manufacturer's instructions as previously described. Briefly, PDAC cells were seeded on cell slides in a 6-well plate, after the treatment of circ-RNA transfection or exosomes addition, cells were incubated with 50 Mm EdU for 2 h, then cells were fixed with 4% paraformaldehyde and permeabilized with 0.5% Triton X-100 for 15 min, then cells were incubated with Click-It reaction mixture for 30 min, the slides were mounted with Mounting Medium for Fluorescence with DAPI (Vector Laboratories, USA) and imaged with a fluorescence microscope.

RNA isolation and qRT-PCR analysis

Cellular RNA was isolated using TRIzol reagent (Thermo, USA) and exosomal RNA was extracted by TRIzol LS (Thermo, USA). First-strand cDNA was generated with PrimeScript RT Reagent Kit with gDNA Eraser (TaKaRa, Japan) and miRNA reverse transcription was performed using a Mir-X miRNA qRT-PCR SYBR Kit (Clontech, Japan). Real-time PCR was performed using the PrimeScript RT Reagent Kit and SYBR Premix Ex Taq (TaKaRa, Japan) on a CFX96 Real-Time System (Bio-Rad, USA) with the reaction conditions provided in the instructions. The primer details used in the study were miR-222 (F: AGCTACATCTGGCTACTGGGT); U6 (F: CTCGCTTCGGCAGCACA, R: AACGCTTCACGAATTTGCGT); p27 (F: TCGGGTCTGTGTCTTTTGG, R: AGACACTCGCACGTTTGACA); beta-actin (F: GCGGACTATGACTTAGTTGCGTTACA, R: TGCTGTACCTTCACCGTTCCA). Additionally, the miRNA mRQ 3' primer was provided in the Mir-X miRNA qRT-PCR SYBR Kit (Clontech, Japan).

Western blot analysis

Total protein of PDAC cells was extracted by RIPA lysis buffer (Thermo, USA) containing protease inhibitor cocktail tablets (Roche, USA) and exosomal protein was isolated using Exosome RNA and Protein Isolation Kit (Thermo, USA). After measured by BCA Protein Assay Kit (Beyotime, China), equal amounts of protein (30 µg) were used to SDS-page on 10% polyacrylamide gels and transferred to PVDF membranes (Millipore, USA), which were blocked and blotted with primary antibodies overnight at 4°C. The antibodies used in this study included the following: anti-p27 (1:800, #3686, CST, USA), anti-p-p27 (1:1000, ab85047, abcam, USA), anti-PPP2R2A (1:1000, #5689, CST, USA), anti-Histone H1 (1:1000, 15446-1-AP, Proteintech, USA), anti-β-actin (1:5000, 20536-1-AP, Proteintech, USA), anti-AKT (1:1000, 4691, Cell Signaling, USA), anti-p-AKT (1:1000, 4060, Cell Signaling, USA) and anti-CD63 (1:500, 10628D, Thermo, USA). The membranes were washed with PBST and incubated with horseradish peroxidase-conjugated secondary antibody for 2 h and the immunocomplexes were then visualized using a New Super ECL Detection Kit (KeyGEN BioTECH, China) according to the manufacturer's protocol.

PDAC patients and clinical samples

A total of 73 patients underwent pancreaticoduodenectomy surgery at Department of Hepatobiliary Surgery Institute, Southwest Hospital, from January 2014 to January 2017. All patients were confirmed to have PDAC by ultrasonography, contrast-enhanced CT or MRI examination and a blood test for markers of digestive system tumors. For the clinical characteristics of these patients, please refer to Table 1. A total

of 43 fresh frozen tissues were used for RNA isolation, fresh tissues were put into liquid-nitrogen immediately after tumor excision and then transferred to -80°C for future use. For plasma exosomes isolation, 10 ml of total blood of each patient was collected and plasma was isolated by a centrifuge 3000 rpm for 20 min. the plasma supernatant was stored at -80°C for future use. Especially, each extracted RNA sample was subjected to an agarose electrophoresis. All patients were followed up by radiography, ultrasonography or CT examination every 3 months after discharge and were followed up monthly by telephone in the clinical follow up center of the Department of Hepatobiliary Surgery Institute, Southwest Hospital. This study was approved by the Ethics Committee of Southwest Hospital, and all patients provided written informed consent.

Animal experiment

All animal experiments were approved by the Institutional Animal Care and Use Committee of Southwest Hospital, Chongqing, China. Briefly, Four- to six-week-old male randomly selected athymic nude mice were obtained from Southwest Hospital (Chongqing, China) and housed in the standard pathogen-free conditions of Southwest Hospital (Chongqing, China). The mice were anesthetized by an intraperitoneal injection of 1% pentobarbital sodium (50 mg/kg). A median abdominal incision was made to expose the spleen and pancreas, and 5×10^6 PDAC cells (in 100 μ l of PBS) were injected to the head of the pancreas. After replacing the pancreas and closing the abdomen, the mice were imaged by the IVIS Lumina II system (Caliper Life Science, USA). All mice were sacrificed at 4 weeks after the procedure, and the pancreas were fixed in 4% paraformaldehyde and subjected to hematoxylin-eosin (H&E) staining.

Dual-luciferase reporter assay

5×10^3 cells were cultured in a white 96-well plate and then transfected with psiCHECK2-circ-PDE8A or psiCHECK2-circ-PDE8A mut plasmid (Sangon Biotech, China) and 8 ng of the internal control pRL-TK Renilla luciferase plasmid (Promega, USA), together with miR-338 (RiboBio, China) or miR-23a (RiboBio, China) at a final concentration of 0, 50 or 150 nM. After a 48-h incubation, the cells were harvested and processed with the Dual-Luciferase Reporter Assay System (E1910, Promega, USA) according to the manufacturer's protocol. The results were quantified as the ratio of firefly luciferase activity/Renilla luciferase activity in each well.

Statistical analysis

The correlation between clinical categorical parameters and plasma exosomal miR-222 expression (the median was regard as cutoff value) was evaluated by a χ^2 test. Student's t-test was used to compare group differences if they followed a normal distribution; otherwise, the nonparametric Mann-Whitney test was adopted. One-way ANOVA was applied to compare the differences among 3 groups. For survival analysis, univariate analysis was conducted by the KM method (the log-rank test), and multivariate analysis was performed by the stepwise Cox multivariate proportional hazard regression model (Forward LR, likelihood ratio). All analyses were performed using SPSS 22.0 software (IBM, USA), all the tests are two-sided and a *P*-value <0.05 was considered to be statistically significant. All statistical analyses were completed under the guidance of experienced experts from the Statistics Department of the Army Medical University.

Table 1. Clinical characteristics and expressions of exosomal miR-222 in 73 pancreatic carcinoma patients

Parameters	miR-222		P-value/ χ^2
	High	Low	
All cases	36	37	
Gender			0.213
Female	9	5	1.553
Male	27	32	
Age, years			0.079
≤60	17	25	3.091
>60	19	12	
Tumor location			0.727
Head	8	7	0.122
Body or tail	28	30	
Tumor size, cm			0.029
≤2	7	16	4.789
>2	29	21	
Neural invasion			0.697
No	23	22	0.151
Yes	13	15	
Duodenal invasion			0.781
No	31	31	0.077
Yes	5	6	
Differentiation			0.047
Low	14	5	6.105
Median	19	28	
High	3	4	
Lymphatic invasion			0.023
No	18	28	5.161
Yes	18	9	
Vascular invasion			0.053
No	23	31	3.751
Yes	13	6	
Liver metastasis			0.303
No	29	33	1.063
Yes	7	4	
T factor			0.047
T1,2	15	24	3.946
T3,4	21	13	
TNM			0.014
I or II A	14	25	6.031
IIB or III, IV	22	12	

Results

The identification of miR-222 in PDAC exosomes

Our previous studies have shown that exosomes from Hs 766T-L2 cells are much more invasive than those from Hs 766T cells. To investigate the possible tumor-related miRNAs in exosomes, we profiled the miRNA expression in exosomes from Hs 766T and Hs 766T-L2 cells. The entire screening procedure is shown in Fig. 1A. Of the dozens of differentially expressed miRNAs, we noted that miR-222 was the most differentially expressed miRNA in tumor exosomes, with a fold-change of 177.72 (Fig. 1B). We next confirmed the high expression levels of miR-222 in exosomes from Hs 766T-L2 cells by qRT-PCR (Fig. 1C). Furthermore, we tested the miR-222 expression in 6 PDAC cell lines and in the normal pancreatic cell lines HPDE and HEK 293. We found that the expression levels of miR-222 were much higher in PDAC cells than those in HPDE or HEK 293 cells (Fig. 1D). To confirm these results, we chose to investigate Hs 766T (the parent cell), Hs 766T-L1, Hs 766T-L2 and Hs 766T-L3 (the daughter cell) cells (Hs 766T-L1, Hs 766T-L2 and Hs 766T-L3 cells are the first, second and third-generation primary tumor cells with increasing invasive ability and derived from a liver metastasis of Hs 766T cells, respectively)[25-27]; as the malignancy of PDAC cells increased, the expression levels of miR-222 also increased successively (Fig. 1E). Thus, we speculate that miR-222 may have an important function in PDAC. We found that the expression levels of miR-222 were the highest in Hs 766T-L3 cells and the lowest in Capan-1 cells (Fig. 1D and 1E); so we further confirmed its upregulation (miR-222 lentivirus) or downregulation (miR-222 shRNA) in Hs 766T-L3, Capan-1 and HEK 293 cells (Fig. 1F). Together, we screened miR-222 in the tumor exosomes and further confirmed that miR-222 was highly expressed in malignant PDAC cells.

miR-222 promotes cell invasion and proliferation in PDAC cells

As miR-222 was highly expressed in malignant cells, we wondered whether miR-222 could promote cell migration or invasion. As expected, wound-healing assays indicated that miR-222 increased the migration of Capan-1 cells, while miR-222 shRNA (si miR-222) decreased the migration of Hs 766T-L3 cells (Fig. 2A-B). Transwell assays also proved that miR-222 promoted cell invasion in Capan-1 and Hs 766T-L3 cells (Fig. 2C-D). To further investigate the role of miR-222 in cell motility, Phalloidin-stained actin filaments were examined in NC or miR-222-overexpressing (ov miR-222) PDAC cells. We found that miR-222 increased the number of filopodia in Capan-1 cells (Fig. 2E and Fig. S1A-B - for all supplemental material see www.karger.com/10.1159/000495281) and the number of lamellipodia in Hs 766T-L3 cells (Fig. 2F and Fig. S1C-D). Furthermore, EdU assays proved that miR-222 overexpression increased cell proliferation in Capan-1 cells (Fig. 2G and Fig. S2A-C), while the miR-222 inhibitor decreased cell proliferation in Hs 766T-L3 cells (Fig. 2H and Fig. S2D-F). We further study the effect of miR-222 on cell cycle; the results indicated that miR-222 overexpression increased the number of cells in G2 or S phase and decreased the number of cells in G1 phase (Fig. 2I). Together, the above results showed that miR-222 could promote cell migration, invasion and proliferation in PDAC cells.

miR-222 regulates the expression and localization of p27

To determine the detailed molecular mechanism of miR-222, we used bioinformatics tools (Miranda and Target Scan) to analyze the possible molecular target. As shown in Fig. 3A, we noted that p27, a classic oncogene, has two 8-mer binding sites for miR-222, and previous studies have reported that p27 can be regulated by miR-222 in Hela cell [28]. Therefore, we further verified the regulation of miR-222 to p27 in PDAC cells. The qRT-PCR results showed that p27 was inhibited by miR-222 overexpression in Capan-1 cells and was overexpressed in Hs 766T-L3 cells treated with a miR-222 shRNA (Fig. 3B). The WB assays also showed similar results (Fig. 3C-D). To confirm this regulation, we constructed wild type or mutated p27 3'UTR firefly luciferase plasmids, in which the two miR-222 binding sites are deleted, the details of these plasmids are shown in Fig. 3E and Table S1. The dual-luciferase reporter

assays showed that co-transfection of wild pGL3 p27 and miR-222 inhibited Rluc expression, this inhibition was dose dependent as the inhibition was more obvious in the 150 nM miR-222 group than in the 50 nM miR-222 group (Fig. 3F, left column). However, these inhibitions were not found in the pGL3 mut-p27 + miR-222 group (Fig. 3F right column).

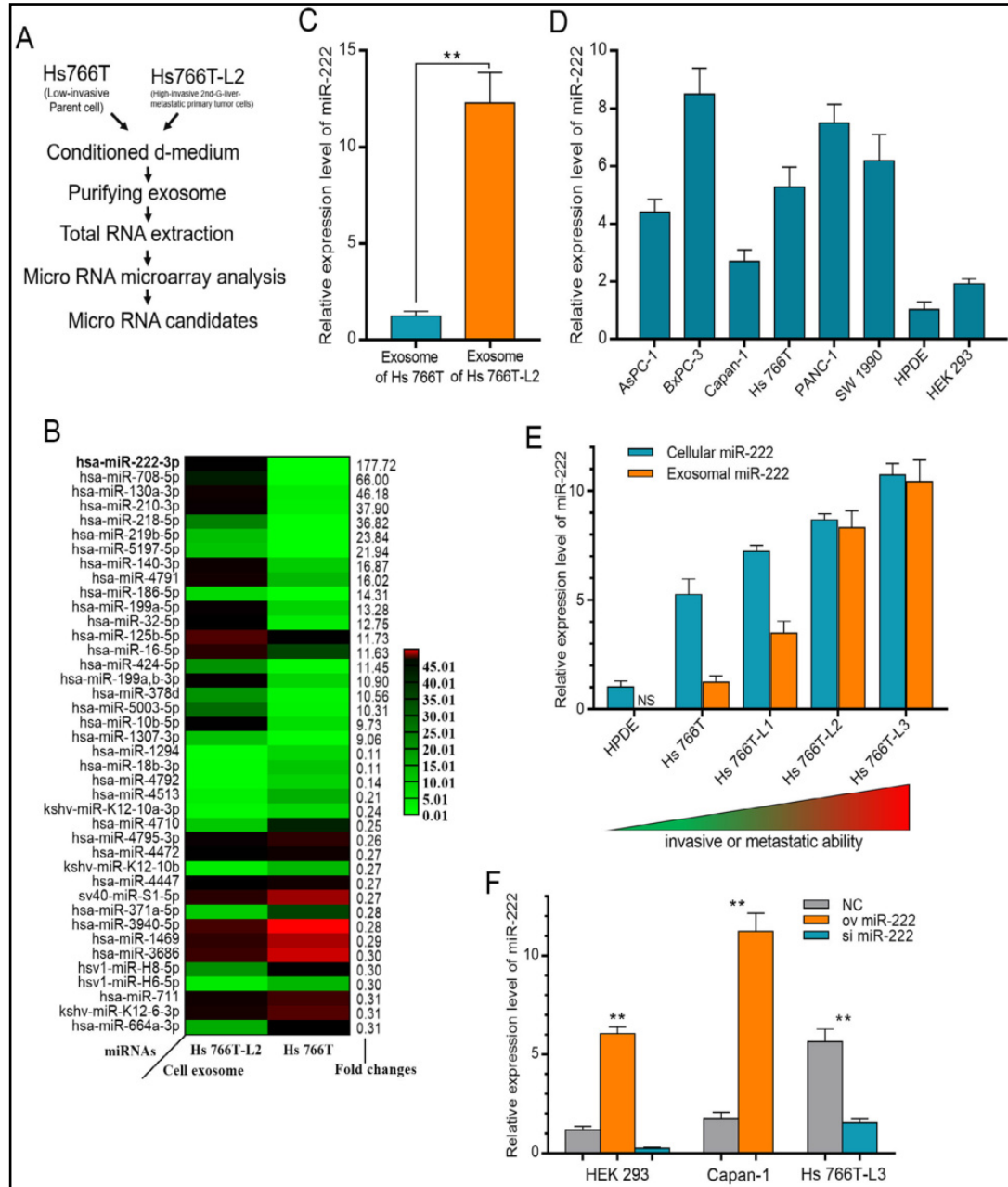


Fig. 1. The identification of miR-222 in PDAC exosomes. (A) The schematic outline of screening miRNA candidates. (B) Heatmap of the screened miRNAs of exosomes from Hs 766T and Hs 766T-L2 cells. Fold change of each screened miRNA was attached in right column. (C) Relative miR-222 expressions of exosomes of Hs 766T and Hs 766T-L2 were measured by qRT-PCR. (D) Relative miR-222 expressions in indicated PDAC or normal cell lines were measured by qRT-PCR. (E) Relative miR-222 expressions in indicated PDAC or normal pancreatic cell lines or their exosomes were measured by qRT-PCR. Cell invasive or metastatic ability was presented in lower column. (F) Relative expressions of miR-222 in indicate treated cells was measured by qRT-PCR. ov miR-222, miR-222 was overexpressed by miR-222 lentivirus; si miR-222, miR-222 was inhibited by miR-222 shRNA. All assays were replicated three times.

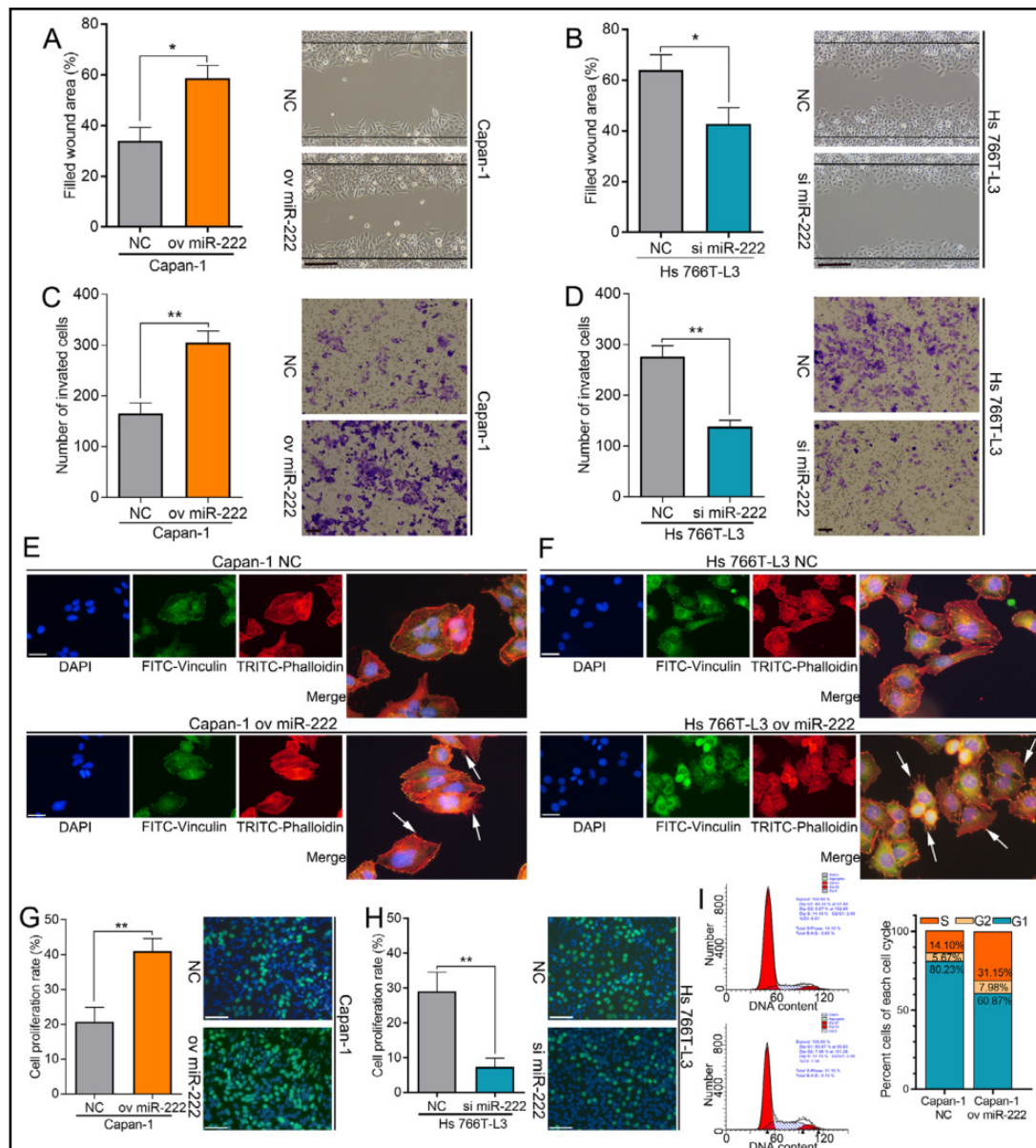


Fig. 2. miR-222 promotes cell invasion and proliferation in PDAC cells. (A-B) The migration abilities of indicate treated Capan-1 (A) or Hs 766T-L3 (B) cells measured by wound-healing assays. Scale bars = 50 μ m. (C-D) The invasion abilities of indicate treated Capan-1 (C) or Hs 766T-L3 (D) cells measured by transwell assays. Scale bars = 50 μ m. (E-F) Representative images of indicate treated Capan-1 (E) or Hs 766T-L3 (F) stained by TRITC-conjugated Phalloidin to indicate actin filaments and counterstained by FITC-conjugated vinculin to show focal contacts. The white arrows indicate the filopodia or lamellipodia. Scale bars = 50 μ m. (G-H) The proliferation abilities of indicate treated Capan-1 (G) or Hs 766T-L3 (H) cells measured by EdU assays. Scale bars = 50 μ m. (I) Representative DNA histogram from control and miR-222 overexpression Capan-1 cells, quantification of the percentage of cells of each cell cycle was showed in right column. All assays were replicated three times.

Next, we confirmed the regulation of miR-222 by p27 in PDAC cells by immunofluorescence assays. First, we confirmed that the expression levels of p27 were obviously higher in Capan-1 cells (Fig. 3G) than in Hs 766T-L3 cells (Fig. 3H), and the results showed that the high expression levels of p27 were inhibited by miR-222 overexpression in Capan-1 cells (Fig. 3I-J). Interestingly, we found that p27 was located primarily in the nucleus in Capan-1

cells (Fig. 3G) but in the cytoplasm in Hs 766T-L3 cells (Fig. 3H); when Capan-1 cells were treated with miR-222, nuclear p27 obviously decreased while cytoplasmic p27 evidently increased (Fig. 3I-J and Fig. S3). Therefore, we measured p27 phosphorylation in miR-222-overexpressing PDAC cells; the WB results showed that miR-222 not only decreased p27 expression levels but also induced p27 phosphorylation in PDAC cells (Fig. 3C-D, the second

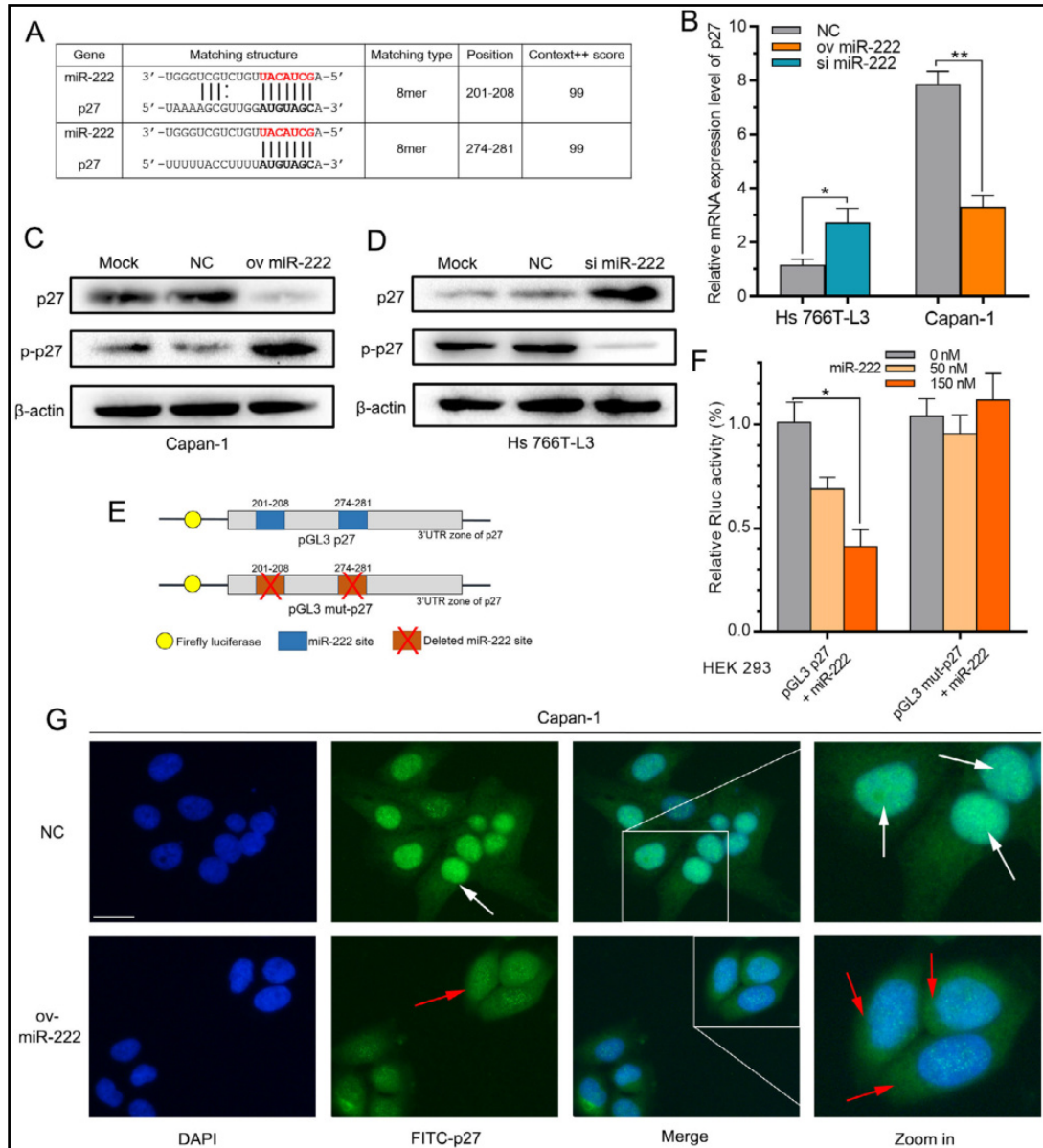


Fig. 3. miR-222 regulates the expression and localization of p27. (A) The prediction for miR-222 binding sites on p-27 transcript. (B) Relative p27 expressions of indicate treated Hs 766T-L2 and Capan-1 were measured by qRT-PCR. (C-D) The protein levels of p27 and p-p27in indicate treated Capan-1 (C) or Hs 766T-L3 (D) cells measured by western blot assays, si miR-222, miR-222 inhibited by miR-222 shRNA. (E) Schematic outlining the wild type and mut p27 luciferase plasmid. (F) Luciferase activity in HEK-293 cells co-transfected with indicate miR-222 concentration or indicate p27 luciferase reporter transcript. Data are showed as the ratio of firefly activity to Renilla luciferase activity. (G-H) The relative protein levels of p27 in Capan-1 (G) or Hs 766T-L3 (H) cells measured by immunofluorescence assays. Scale bars = 50 μ m. (I-J) The relative protein levels of p27 in indicate treated Capan-1 cells measured by immunofluorescence assays. Scale bars = 50 μ m. All assays were replicated three times.

column). Together, we found that miR-222 could decrease p27 expression levels and increase p27 phosphorylation, which may induce the increasing cytoplasmic p27 expression.

miR-222 promotes p27 phosphorylation via activating AKT

Next, we investigated how miR-222 promoted AKT phosphorylation. As several studies reported that miR-222 could activate AKT through inhibiting PPP2R2A [29], we verified the result in PDAC. As expected, WB results showed that miR-222 inhibited the expression of PPP2R2A in Capan-1 and Hs 766T-L3 cells (Fig. 4A-B). Further studies confirmed that miR-

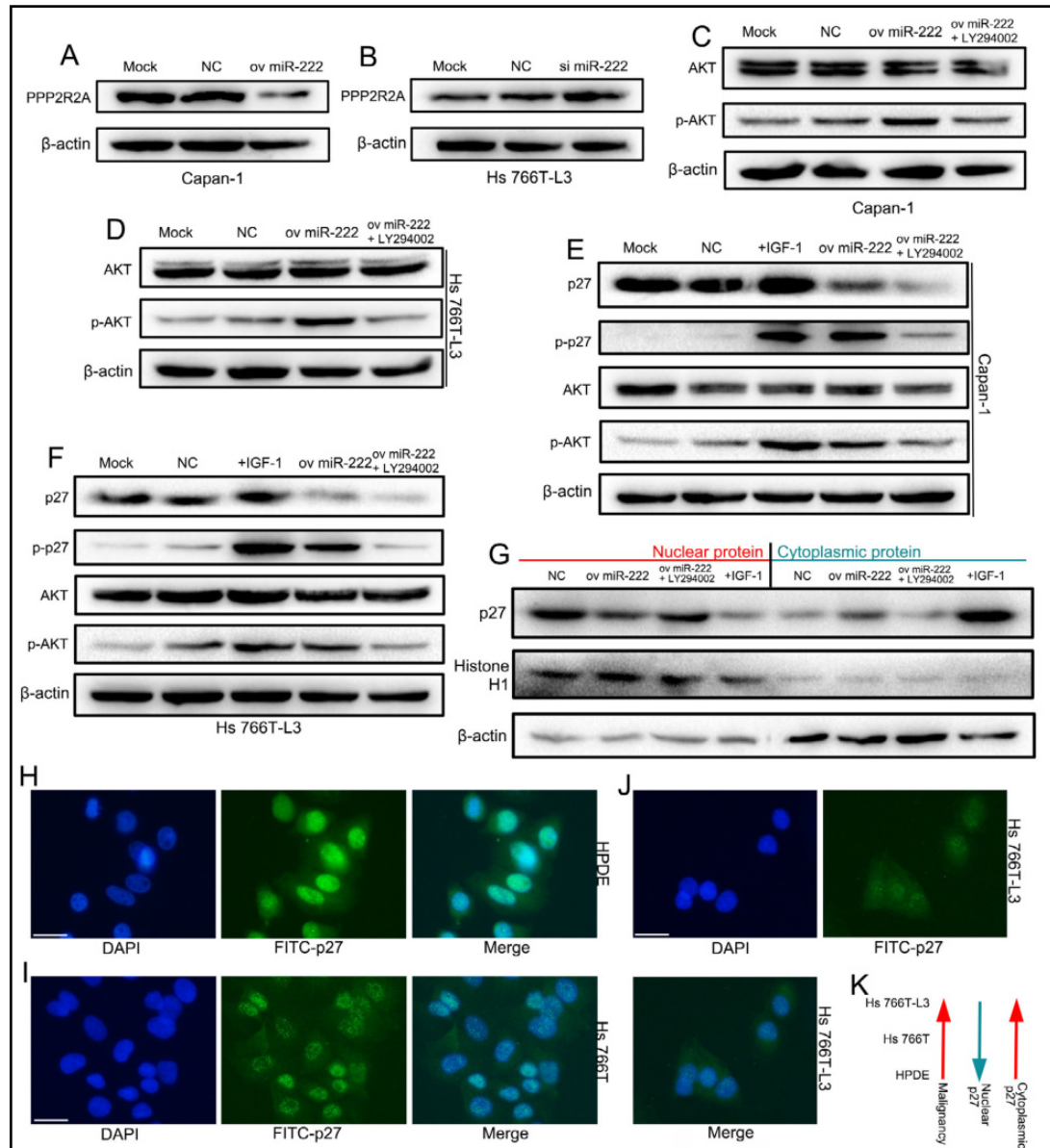


Fig. 4. miR-222 promotes p27 phosphorylation via activating AKT. (A-B) The protein level PPP2R2A in indicate treated Capan-1 (A) or Hs 766T-L3 (B) cells. (C-D) The protein levels of AKT and p-AKT in indicate treated Capan-1 (C) or Hs 766T-L3 (D) cells. LY294002, the AKT phosphorylation inhibitor. (E-F) The protein levels of p-27, p-p27, AKT and p-AKT in indicate treated Capan-1 (E) or Hs 766T-L3 (F) cells. (G) The nuclear and cytoplasmic protein of indicate treated Capan-1 cells were separated and protein level of p27 was analyzed by WB analysis. (H-K) The relative protein levels of p27 in indicate cells measured by immunofluorescence assays. Scale bars = 50 μ m. All assays were replicated three times.

222 activated AKT by promoting its phosphorylation, to confirm the AKT phosphorylation (i.e. AKT activation) results, we treated cells with LY294002, an AKT inhibitor, and found that miR-222-induced AKT phosphorylation was inhibited by LY294002 (Fig. 4C-D).

The results above showed that miR-222 could activate AKT and promote p27 phosphorylation; thus, we wondered whether miR-222 promoted p27 phosphorylation via activating AKT. An AKT activator (IGF-1) and inhibitor (LY294002) were used in this study. We found that LY294002 did not affect the p27 phosphorylation in untreated PDAC cells (data not shown); further research showed that AKT could be activated by IGF-1 and miR-222, but AKT phosphorylation levels were higher in the IGF-1 group than in the miR-222 group. In addition, the AKT activation induced by miR-222 was further blocked by the addition of LY294002. These results were confirmed in both Capan-1 and Hs 766T-L3 cells (Fig. 4E-F).

Previous studies revealed that p27 could be phosphorylated by AKT at T-157, which further affect the expression localization of p27 [30, 31]. Next, we studied the relationship between AKT and p27 phosphorylation and the localization of p27. Capan-1 cells were treated with IGF-1, miR-222 or LY294002, and the nuclear and cytoplasmic proteins of each group were separated by special kits; the WB results showed that the majority of p27 was indeed expressed in the nucleus in the NC group. Once the cells were treated with IGF-1 or miR-222, p27 was highly expressed in the cytoplasm instead of in the nucleus. However, when Capan-1 cells were treated with miR-222 and LY294002, the expression of p27 in the cytoplasm was decreased (Fig. 4G).

Furthermore, because miR-222 is related to tumor progression and miR-222-overexpressing Capan-1 cells expressed more cytoplasmic p27 than the untreated cells, we suggest that in contrast to nuclear p27, cytoplasmic p27 is associated with tumor malignancy. The immunofluorescence results showed that the cytoplasm levels of p27 in cells, ranked from low to high, are HPDE, Hs 766T and Hs 766T-L3 cells; the nuclear p27 levels were opposite (Fig. 4H-K). Together, our results showed that miR-222 promotes p27 phosphorylation via activating AKT, which increases the cytoplasmic p27 expression and tumor progression.

miR-222 promotes tumor progression in vivo

Our results above showed that miR-222 expression in PDAC cells, ranked from high to low, was Hs 766T-L3, Hs 766T-L2, Hs 766T-L1, Hs 766T and HPDE cells. We next measured their p27 expression. Interestingly, their p27 expression levels were the opposite of their miR-222 expression levels (Fig. 5A). To confirm this result *in vivo*, we analyzed the expression levels of miR-222 and p27 in 43 clinical pancreatic tumor samples. Similarly, we found that the expression levels of miR-222 and p27 were significantly inversely correlated ($r=-4.14$, $p=0.006$) (Fig. 5B).

We next studied the role of miR-222 in *in vivo* conditions. Capan-1 NC cells (NC) or stable miR-222-overexpressing Capan-1 cells (ov miR-222) were injected into the head of the pancreas of nude mice. The pancreatic tumor of each mouse was analyzed every week by a luciferase IVIS system (Fig. 5C). The *in vivo* imaging results showed that the luciferase intensity of the ov miR-222 group was significantly higher than that of the NC group (Fig. 5D and E). A month later, the pathological examination results showed that the pancreatic tumors of the ov miR-222 group were obviously larger than those of the NC group (Fig. 5F-H).

Imaging exosome communication in PDAC cells

As we screened miR-222 in tumor exosomes, we next studied the exosome communication in PDAC cells. First, exosomes of Hs 766T-L3 were confirmed by TEM analysis (Fig. 6A). Calcein-AM-labeled Capan-1 cells were cocultured with Dil-labeled exosomes (purified from the conditioned medium of Hs 766T-L3 cells) for 24 h, and the live cells were observed with a fluorescence microscope; the results showed dotted, red exosome signals in the cytoplasm of Capan-1 cells (Fig. 6B and Fig. S4A). To further confirm these results, we labeled exosomes

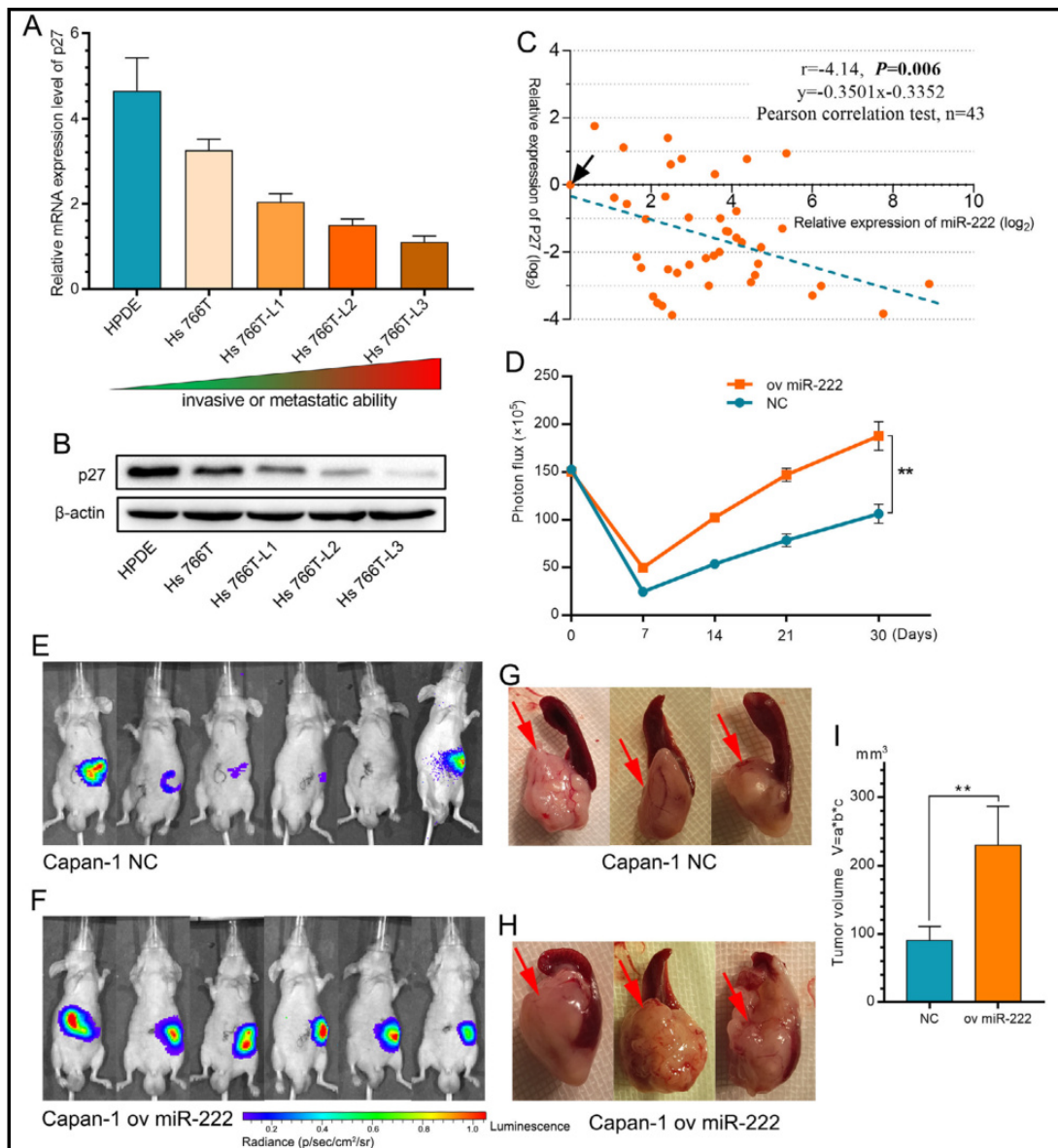


Fig. 5. miR-222 promotes tumor progression in vivo. (A) Relative p27 mRNA expressions in indicated PDAC or normal cell lines were measured by qRT-PCR. (B) Relative p27 protein expressions in indicated PDAC or normal cell lines were measured by WB assay. (C) The correlation analysis of p27 and miR-222 in 43 tissues of PDAC patients, the black arrow indicates the control sample. (D-I) Animal experiments, the luciferase intensities were measured each week (D) after intrapancreatic injection with NC (E) or ov miR-222 (F) Capan-1 cells, pancreatic tumor in situ (the red arrows point to) were showed by autopsy (G-H), tumor size of each group was measured by tumor volume (I). All assays were replicated three times.

from Hs 766T-L3 cells with CD63-GFP lentivirus to form stable GFP-CD63-Hs 766T-L3 (exo-Hs 766T-L3) cells. In addition, RFP-labeled Capan-1 cells were cocultured with exosomes from exo-Hs 766T-L3 cells. The fluorescence assays showed similar results above; green, dotted exosome signals were also located in the cytoplasm of Capan-1 cells (Fig. 6C and Fig. S4B). To confirm that the dotted signals were exosomes, Capan-1 cells were cocultured with Dil-labeled exosomes to establish the immunofluorescence of CD63, an exosome marker. Confocal microscopy analyses showed that the Dil-labeled exosomes and FITC-labeled CD63 signals were found in the cytoplasm, and the distribution and morphology of these two types of fluorescence signals were almost identical (Fig. 6D).

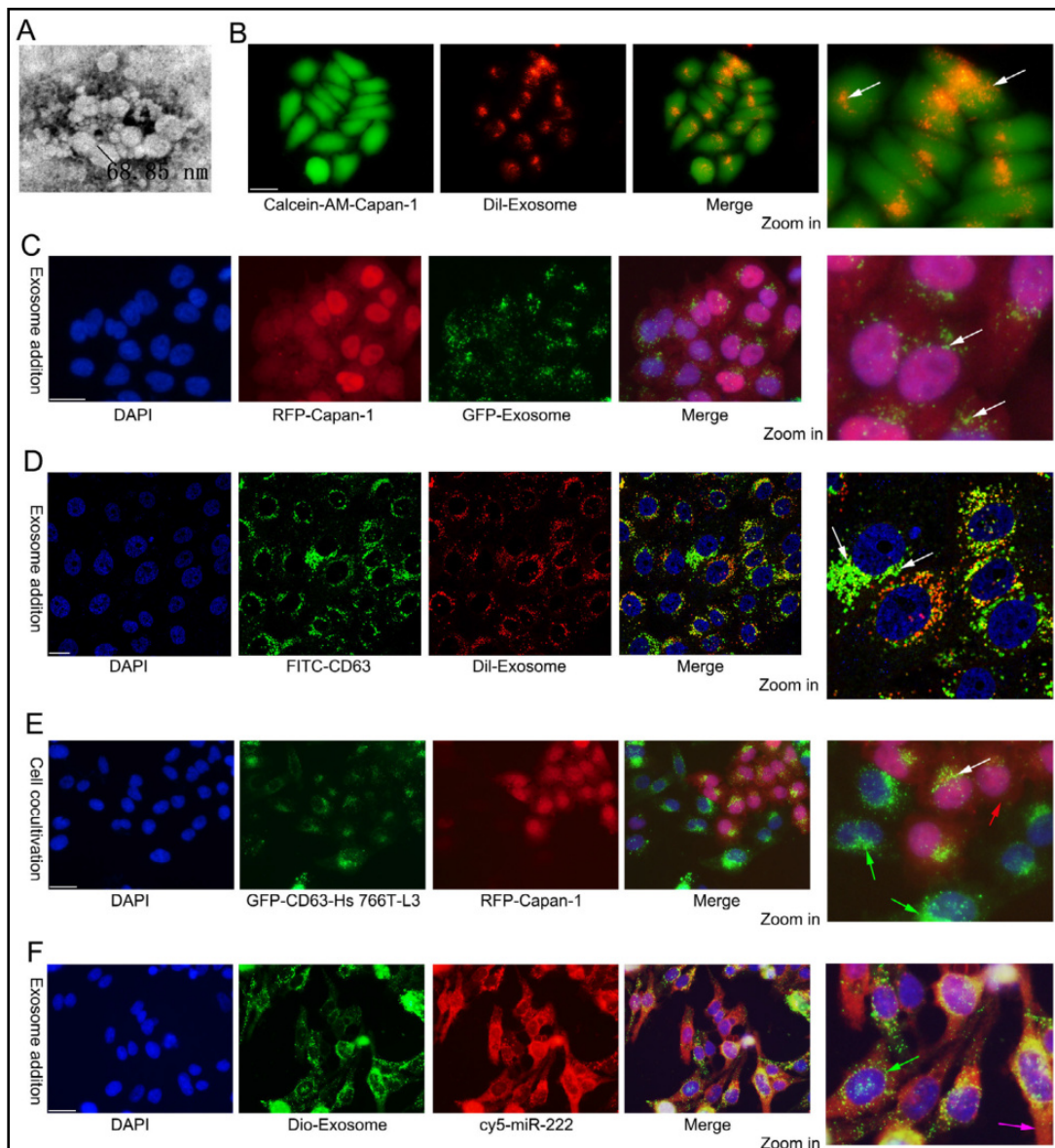


Fig. 6. Imaging exosome communication in PDAC cells. (A) Exosomes from cell medium of Hs 766T-L3 were validated by TEM to validate their morphology. (B) Dil labeled exosomes were added into Calcein AM labeled Capan-1 cells for co-cultivation, images were captured with fluorescence microscope, the white arrows indicate exosomes. Scale bars = 25 μ m. (C) Exosomes of GFP-CD63-Hs 766T-L3 were purified and added into RFP labeled Capan-1 cells for co-cultivation, images were captured with fluorescence microscope, the white arrows indicate exosomes. Scale bars = 25 μ m. (D) Dil labeled exosomes were added into Capan-1 cells, then the locations of CD63 or Dil labeled exosomes were analyzed by confocal microscope. Scale bars = 12.5 μ m. (E) RFP-labeled Capan-1 cells were co-cultured with GFP-CD63-Hs 766T-L3, then images were captured with fluorescence microscope. Scale bars = 25 μ m. The white arrow indicates exosomes, the red arrows indicate the receipt cells and the green arrows indicate exosome-releasing cells. (F) Dio labeled exosomes of ov cy5-miR-222 Hs 766T-L3 were added into Capan-1 cells for co-cultivation, images were captured with fluorescence microscope, the green arrow indicates exosomes and pink arrow indicates cy5-miR signals. Scale bars = 25 μ m. All assays were replicated three times.

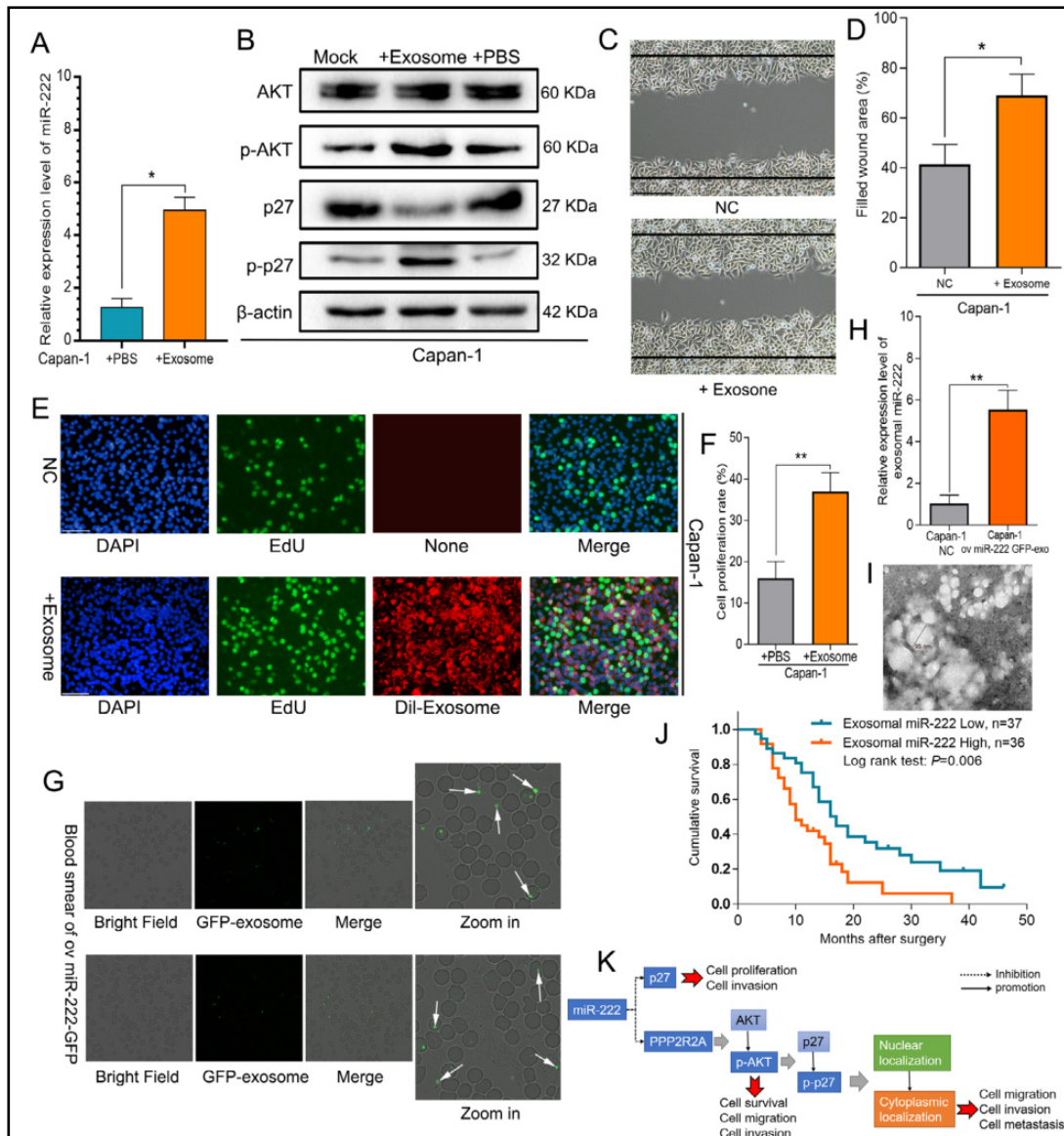


Fig. 7. Exosomal miR-222 is an independent risk factor for PDAC patient survival. (A) The relative expression of miR-222 in indicate treated Capan-1 cells measured by qRT-PCR, +exosomes, addition of exosomes of ov miR-222-Hs 766T cells. (B) Protein levels of AKT, p-AKT, p27 and p-p27 of indicate treated Capan-1 cells measured by WB assay. (C-D) The migration abilities of indicate treated Capan-1 cells measured by wound-healing assays, +Exosomes, addition of exosomes of ov miR-222-Hs 766T cells. Scale bars = 50 μ m. (E-F) The proliferation abilities of indicate treated Capan-1 cells measured by EdU assays. Scale bars = 50 μ m. (G-H) Exosome in vivo experiment, Capan-1 (NC) or miR-222 overexpressed GFP-exo Capan-1 (i.e. miR-222 and GFP-CD63 lentiviruses co-transfected Capan-1 cells) cells were injected into pancreatic of nude mice to form tumor in situ, the tumor-released exosomes were identified in blood by confocal microscope (G). Scale bars = 50 μ m; and plasma exosomal miR-222 expression was measured by qRT-PCR (H). (I) Representative image of plasma exosomes of clinical PDAC patients. (J) KM survival curves for the overall survival of 73 PDAC patients according to the relative expression of plasma exosomal miR-222 Expression. (K) The schematic outline of the roles of miR-222 in PDAC. All assays were replicated three times.

Furthermore, RFP-labeled Capan-1 and exo-Hs 766T-L3 cells were mixed together at a 1:1 ratio for a 48-h co-cultivation; the fluorescence results also showed green, dotted exosomal signals in the cytoplasm of the red Capan-1 cells (Fig. 6E and Fig. S4C). To confirm the transmission of miR-222 between PDAC cells via exosomes, Hs 766T-L3 cells were transfected with cy5-miR-222. Two days later, the cells were washed with PBS, and the cell exosomes (labeled with Dio dye) were purified from the medium a day later; then, the exosomes were added to Capan-1 cells for a 24-h co-cultivation. The fluorescence results showed red miR-222 signals and green, dotted exosomal signals (Fig. 6F and Fig. S4D). Together, these data confirm the transmission of miR-222 between PDAC cells via exosomes.

Exosomal miR-222 is an independent risk factor for PDAC patient survival

We confirmed exosomal miR-222 transmission between PDAC cells; next, we wondered whether the miR-222 transmission was functional. Thus, exosomes from miR-222-overexpressing Hs 766T-L3 cells were purified and added to Capan-1 cells (+exosome group) for qRT-PCR and WB analysis. The results showed that compared with the addition of PBS (NC group), the addition of miR-222 exosomes increased the miR-222 expression (Fig. 7A), and induced the phosphorylation of AKT and p27 and decreased p27 expression levels (Fig. 7B). Transwell (Fig. 7C-D) and EdU (Fig. 7E-F) assays also showed that the addition of miR-222 exosomes promoted the proliferation of Capan-1 cells. To further study the tumor released exosomes *in vivo* conditions, Capan-1 cells were transfected by miR-222 and GFP-CD63 lentiviruses together and injected to pancreas to form pancreatic cancer in mice. A month later, we did the peripheral blood (from tail vein) smear test, and under the confocal microscopy analysis we identified the green GFP signals, which were mainly located in red cells (Fig. 7G), the results suggest that tumor secreted exosomes could enter into blood circulation system. Furthermore, we found that the expression level of miR-222 was elevated compared to NC group mice (Fig. 7H).

These results above suggest that exosomal miR-222 may play important roles in PDAC; next, we collected plasma from 73 clinical PDAC patients. The exosomes were purified, and confirmed by TEM (Fig. 7I), and exosomal RNA was extracted from these samples for miR-222 analysis. We found that exosomal miR-222 was significantly associated with tumor size, tumor differentiation and TNM stage (Table 1). A survival analysis revealed that exosomal miR-222 was related to low survival rates in PDAC patients (Fig. 7J), and multivariate analyses showed that both exosomal miR-222 and TNM stage were independent risk factors for PDAC survival (Table 2).

Based on our above results, we summarized the role of miR-222 in PDAC (Fig. 7K). miR-222 has two roles in PDAC: on the one hand, miR-222 decreases p27 expression to induce cell invasion and proliferation; on the other hand, miR-222 inhibits PPP2R2A and activates AKT, which led to p27 phosphorylation and cytoplasmic p27 expression. These effects induced cell survival, invasion and metastasis. In addition, miR-222 can be transmitted via exosomes, and this transmission is functional.

Discussion

In this study, we identified miR-222 using a microarray analysis of exosomes from highly metastatic PDAC cells. Further research revealed that miR-222 could directly regulate

Table 2. Univariate and multivariate survival analyses of the prognostic factors associated with survival in pancreatic carcinoma patients (n=73)

OS	Univariate analysis			Multivariate analyses		
	Patients, n	Median survival time	P-value	HR	95% CI	P-value
Gender, Male/Female	14/59	14/15	0.212			
Age, ≤60/>60	42/31	16/13	0.138			
Tumor location, head/body or tail	15/58	10/16	0.132			
Tumor size, ≤2/>2	23/50	17/12	0.072			
Duodenal invasion, Yes/No	62/11	16/8	0.309			
Differentiation, Low/Median/High	19/47/7	11/15/42	0.138			
Lymphatic invasion, Yes/No	46/27	15/12	0.069			
Vascular invasion, Yes/No	54/19	16/9	0.029			
Liver metastasis, Yes/No	62/11	16/9	0.01			0.419
TNM, I, IIA/ IIB, III or IV	39/34	16/11	0.004	1.921	1.079-3.420	0.027
miR-222, High/Low	37/36	17/10	0.006	1.767	1.009-3.094	0.046

p27 to promote cell proliferation and invasion and could also activate AKT by inhibiting PPP2R2A expression, thus inducing p27 phosphorylation and cytoplasmic p27 expression to promote cell survival, invasion and metastasis. Interestingly, these processes could be mediated by exosome transmission. We also measured plasma exosomal miR-222 in 73 PDAC patients and found that exosomal miR-222 is associated with tumor progression and is an independent risk factor for PDAC survival.

Recently, many studies of tumor-related miRNAs in different types of tumors have emerged; different miRNAs have been reported to modulate almost all physiological processes of tumor initiation, invasion, and metastasis [32, 33]. In PDAC, similar to other tumors, the majority of tumor-related miRNAs are tumor suppressors; for example, the miR-200 family was found to be downregulated and play important roles in EMT, cell proliferation and apoptosis [34]. Other tumor suppressors include miR-26, miR-34a, and miR-192 [35]. Oncogenic miRNAs are relatively scarce. Some of the reasons include that oncogenes are preferentially analyzed in tumor studies, and miRNAs regulate gene expression mainly by degrading mRNA or suppressing translation. In this study, we measured miR-222 levels and found that they were closely related to tumor malignancy. Further study revealed that miR-222 could inhibit the expression of p27, a key cell-cycle regulator. Interestingly, we generated a series of PDAC cells with different metastatic abilities, Hs 766T (parent cells) to Hs 766T-L3 cells, which are the third-generation primary cells of a metastatic liver tumor. We found that miR-222 expression levels increased successively when p27 expression levels decreased successively. In PDAC samples, miR-222 expression levels were also inversely correlated with those of p27. Thus, the expression of miR-222, an oncogenic gene, was confirmed in PDAC. Our results were also consistent with other studies of HCC or bladder cancer [29, 36].

Recently, more and more studies indicate that changes in gene localization could result in different or even opposite biological functions. For example, cytoplasmic and nuclear PCBP1 were reported to have different regulatory functions [37]; KLF4, which is primarily located in the nucleus and functions as a tumor suppressor, exerts oncogenic effects when expressed in the cytoplasm [38]. We suggest that p27 also has opposite functions when its cellular distribution changes in PDAC. First, consistent with our results, p27 acts as a tumor suppressor when located in the nucleus; we found that normal or slightly malignant cells, such as HEK 293, HPDE, Capan-1 and Hs 766T cells, all express high levels of p27 in the nucleus. Second, in highly malignant cells, such as Hs 766T-L3 cells, low levels of p27 are expressed, but p27 is mainly located in the cytoplasm. Our results are in line with those of Catherine Denicourt's melanoma study [39]; in this study, the re-localization of p27 to the cytoplasm was closely related to tumor invasion or metastasis rather than to tumor suppression, as when it was originally localized to the nucleus in melanoma. We investigated the possible mechanisms of p27 re-localization and found that activated AKT induced p27 phosphorylation, thus leading to high levels of cytoplasmic p27 expression; these results were further confirmed by WB using proteins from the nuclear and cytoplasmic protein separation assays. Furthermore, it should be noted that the total p27 expression seems to be negatively associated with tumor malignancy; possible reasons for this include that the majority of tumor cells express p27 in the nucleus, and cytoplasmic p27 levels in highly malignant cells are low. The results above may be important for the clinical application of p27 therapies in the future: if p27 is distributed mainly to the cytoplasm in some patients, p27 therapeutics may fail.

Exosomes are regarded as stable and effective carriers between different tumor cells, and different tumor-related nucleic acids or proteins in exosomes were found to play diagnostic or regulatory roles [40, 41]. Our research revealed that tumor cells can transfer miR-222 to other cells via exosomes to increase malignancy; these results are different from those of some other studies [42]. First, we screened miR-222 in tumor exosomes rather than in tumor tissue, and the experimental cell lines were highly metastatic daughter cells of the control cells. Second, we used many different experiments to confirm exosome transfer, and exosomal miR-222 transfer was confirmed and imaged. Third, we showed that exosomal miR-222 transfer between PDAC cells was functional. Finally, we analyzed plasma exosomal miR-222 expression

in clinical PDAC patients and discovered that exosomal miR-222 was associated with tumor progression and prognosis. Furthermore, it has been reported that exosomes can protect their inner miRNAs from degradation [43]. In addition, plasma exosomes are relatively easy to collect (via blood draw); thus, we believe that detecting biomolecules in exosomes is convenient and effective. Exosomal miR-222 may play important diagnostic roles in PDAC.

Based on the data we described above, we proposed our hypothesis of the role of exosomal miR-222 in PDAC (Fig. 8): Normal or slightly malignant cells expressed less miR-222 but more nuclear p27, once they received exosomes containing high levels of miR-222 that were released from malignant tumor cells, Slightly malignant cells exerted at least two biological effects: on the one hand, the total p27 expression was inhibited; on the other hand, the miR-222/PPP2R2A/AKT pathway was activated to phosphorylate p27, that leading to cytoplasmic p27 expression. These effects resulted in cell proliferation, invasion and metastasis. Furthermore, miR-222 can enter into blood circulation via exosome communication and be detected in clinical practice.

Conclusion

We screened oncogenic miR-222 from tumor exosomes via microarray analysis and revealed that miR-222 regulates p27 expression; we also found that miR-222 could phosphorylate p27 via the miR-222/PPP2R2A/AKT pathway to re-localize p27. Exosomal miR-222 transfer was also confirmed *in vitro*, and exosomal miR-222 expression was correlated with tumor progression and prognosis. Thus, exosomal miR-222 may play important regulatory and diagnostic roles in PDAC.

Abbreviations

miRNAs (MicroRNAs); PDAC (pancreatic ductal adenocarcinoma); p27 (p27 Kip1); d-FBS (exosomes-depleted FBS).

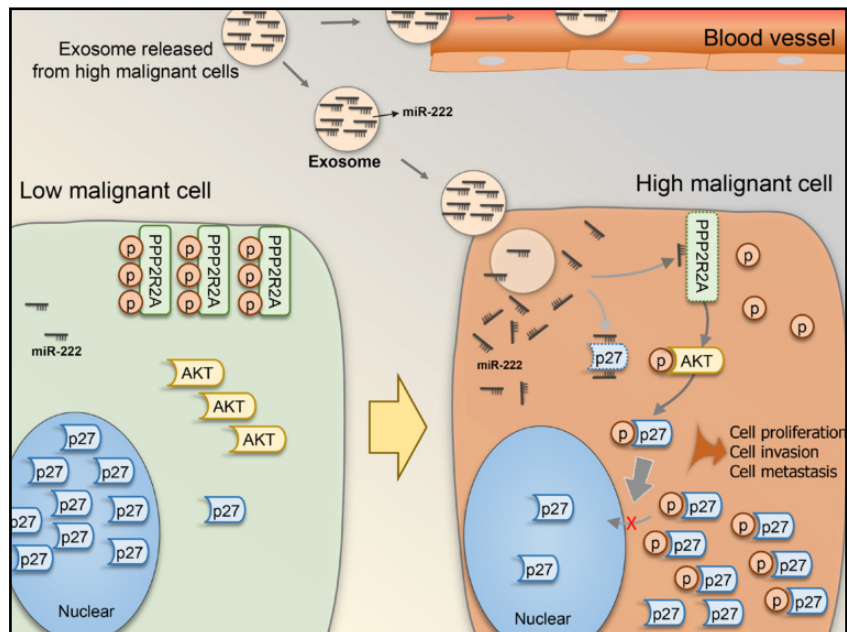


Fig. 8. A schematic model of exosomal miR-222 functions during tumor invasion.

Acknowledgements

Zhonghu Li, Xiaowu Li and Xiangde Liu designed the experiments. Zhonghu Li and Yang Tao performed the experiments. Xiaoya Wang, Jie Li, Peng Jiang, Minjie Peng, Xi Zhang, Kai Chen, Hui Liu, Jin Zhu and Ping Zhen collected the clinical samples and analyzed the data. Zhonghu Li prepared figures and drafted the manuscript. Xiaowu Li provided the financial support and supervised laboratorial processes. All authors read and approved the final manuscript.

This work was mainly supported by the National Natural Science Foundation of China under Grant 81430063. Part of work was also supported by the Scientific Research Project of North Sichuan Medical College (CBY17-A-YB39) and the Science and Technology Project of the Health Planning Committee of Sichuan (18PJ430).

We thank professors of Statistics Department, Military Preventive Medicine, Army Medical University for the statistical help!

Disclosure Statement

The authors declare that they have no competing interests.

References

- 1 Hidalgo M: Pancreatic cancer. *N Engl J Med* 2010;362:1605-1617.
- 2 Siegel RL, Miller KD, Jemal A: Cancer Statistics, 2017. *CA Cancer J Clin* 2017;67:7-30.
- 3 Renz BW, Boeck S, Roeder F, Trumm C, Heinemann V, Werner J: Oligometastatic Disease in Pancreatic Cancer - How to Proceed? *Visc Med* 2017;33:36-41.
- 4 Hartwig W, Werner J, Jager D, Debus J, Buchler MW: Improvement of surgical results for pancreatic cancer. *Lancet Oncol* 2013;14:e476-485.
- 5 Fidler IJ: The pathogenesis of cancer metastasis: the 'seed and soil' hypothesis revisited. *Nat Rev Cancer* 2003;3:453-458.
- 6 Sharma SS, Pledger WJ: The non-canonical functions of p27(Kip1) in normal and tumor biology. *Cell Cycle* 2016;15:1189-1201.
- 7 Polyak K, Kato JY, Solomon MJ, Sherr CJ, Massague J, Roberts JM, Koff A: p27Kip1, a cyclin-Cdk inhibitor, links transforming growth factor-beta and contact inhibition to cell cycle arrest. *Genes Dev* 1994;8:9-22.
- 8 Laplante M, Sabatini DM: mTOR signaling at a glance. *J Cell Sci* 2009;122:3589-3594.
- 9 Uddin S, Hussain AR, Al-Hussein KA, Manogaran PS, Wickrema A, Gutierrez MI, Bhatia KG: Inhibition of phosphatidylinositol 3'-kinase/AKT signaling promotes apoptosis of primary effusion lymphoma cells. *Clin Cancer Res* 2005;11:3102-3108.
- 10 Zhang H, Bai M, Deng T, Liu R, Wang X, Qu Y, Duan J, Zhang L, Ning T, Ge S, Li H, Zhou L, Liu Y, Huang D, Ying G, Ba Y: Cell-derived microvesicles mediate the delivery of miR-29a/c to suppress angiogenesis in gastric carcinoma. *Cancer Lett* 2016;375:331-339.
- 11 Filipowicz W, Bhattacharyya SN, Sonenberg N: Mechanisms of post-transcriptional regulation by microRNAs: are the answers in sight? *Nat Rev Genet* 2008;9:102-114.
- 12 Kallen AN, Zhou XB, Xu J, Qiao C, Ma J, Yan L, Lu L, Liu C, Yi JS, Zhang H, Min W, Bennett AM, Gregory RI, Ding Y, Huang Y: The imprinted H19 lncRNA antagonizes let-7 microRNAs. *Mol Cell* 2013;52:101-112.
- 13 He L, Hannon GJ: MicroRNAs: small RNAs with a big role in gene regulation. *Nat Rev Genet* 2004;5:522-531.
- 14 Tie J, Fan D: Big roles of microRNAs in tumorigenesis and tumor development. *Histol Histopathol* 2011;26:1353-1361.
- 15 Kim J, Yao F, Xiao Z, Sun Y, Ma L: MicroRNAs and metastasis: small RNAs play big roles. *Cancer Metastasis Rev* 2017;10.1007/s10555-017-9712-y.
- 16 Trebicka J, Anadol E, Elfimova N, Strack I, Roggendorf M, Viazov S, Wedemeyer I, Drebber U, Rockstroh J, Sauerbruch T, Dienes HP, Odenthal M: Hepatic and serum levels of miR-122 after chronic HCV-induced fibrosis. *J Hepatol* 2013;58:234-239.

- 17 Azmi AS, Bao B, Sarkar FH: Exosomes in cancer development, metastasis, and drug resistance: a comprehensive review. *Cancer Metastasis Rev* 2013;32:623-642.
- 18 Vader P, Breakefield XO, Wood MJ: Extracellular vesicles: emerging targets for cancer therapy. *Trends Mol Med* 2014;20:385-393.
- 19 Moore C, Kosgodage U, Lange S, Inal JM: The emerging role of exosome and microvesicle- (EMV-) based cancer therapeutics and immunotherapy. *Int J Cancer* 2017;141:428-436.
- 20 Sheridan C: Exosome cancer diagnostic reaches market. *Nat Biotechnol* 2016;34:359-360.
- 21 Marleau AM, Chen CS, Joyce JA, Tullis RH: Exosome removal as a therapeutic adjuvant in cancer. *J Transl Med* 2012;10:134.
- 22 Joyce DP, Kerin MJ, Dwyer RM: Exosome-encapsulated microRNAs as circulating biomarkers for breast cancer. *Int J Cancer* 2016;139:1443-1448.
- 23 Zaharie F, Muresan MS, Petrushev B, Berce C, Gafencu GA, Selicean S, Jurj A, Cojocneanu-Petric R, Lisencu CI, Pop LA, Pileczki V, Eniu D, Muresan MA, Zaharie R, Berindan-Neagoe I, Tomuleasa C, Irimie A: Exosome-Carried microRNA-375 Inhibits Cell Progression and Dissemination via Bcl-2 Blocking in Colon Cancer. *J Gastrointest Liver Dis* 2015;24:435-443.
- 24 Umezu T, Ohyashiki K, Kuroda M, Ohyashiki JH: Leukemia cell to endothelial cell communication via exosomal miRNAs. *Oncogene* 2013;32:2747-2755.
- 25 Li Z, Jiang P, Li J, Peng M, Zhao X, Zhang X, Chen K, Zhang Y, Liu H, Gan L, Bi H, Zhen P, Zhu J, Li X: Tumor-derived exosomal Inc-Sox2ot promotes EMT and stemness by acting as a ceRNA in pancreatic ductal adenocarcinoma. *Oncogene* 2018;37:3822-3838.
- 26 Li Z, Yanfang W, Li J, Jiang P, Peng T, Chen K, Zhao X, Zhang Y, Zhen P, Zhu J, Li X: Tumor-released exosomal circular RNA PDE8A promotes invasive growth via the miR-338/MACC1/MET pathway in pancreatic cancer. *Cancer Lett* 2018;432:237-250.
- 27 Zou Y, Li J, Chen Z, Li X, Zheng S, Yi D, Zhong A, Chen J: miR-29c suppresses pancreatic cancer liver metastasis in an orthotopic implantation model in nude mice and affects survival in pancreatic cancer patients. *Carcinogenesis* 2015;36:676-684.
- 28 le Sage C, Nagel R, Egan DA, Schrier M, Mesman E, Mangiola A, Anile C, Maira G, Mercatelli N, Ciafre SA, Farace MG, Agami R: Regulation of the p27(Kip1) tumor suppressor by miR-221 and miR-222 promotes cancer cell proliferation. *EMBO J* 2007;26:3699-3708.
- 29 Wong QW, Ching AK, Chan AW, Choy KW, To KF, Lai PB, Wong N: MiR-222 overexpression confers cell migratory advantages in hepatocellular carcinoma through enhancing AKT signaling. *Clin Cancer Res* 2010;16:867-875.
- 30 Zhao D, Besser AH, Wander SA, Sun J, Zhou W, Wang B, Ince T, Durante MA, Guo W, Mills G, Theodorescu D, Slingerland J: Cytoplasmic p27 promotes epithelial-mesenchymal transition and tumor metastasis via STAT3-mediated Twist1 upregulation. *Oncogene* 2015;34:5447-5459.
- 31 Liang J, Zubovitz J, Petrocelli T, Kotchetkov R, Connor MK, Han K, Lee JH, Ciarallo S, Catzavelos C, Beniston R, Franssen E, Slingerland JM: PKB/Akt phosphorylates p27, impairs nuclear import of p27 and opposes p27-mediated G1 arrest. *Nat Med* 2002;8:1153-1160.
- 32 Gurtner A, Falcone E, Garibaldi F, Piaggio G: Dysregulation of microRNA biogenesis in cancer: the impact of mutant p53 on Drosha complex activity. *J Exp Clin Cancer Res* 2016;35:45.
- 33 Croston TL, Lemons AR, Beezhold DH, Green BJ: MicroRNA Regulation of Host Immune Responses following Fungal Exposure. *Front Immunol* 2018;9:170.
- 34 Herreros-Villanueva M, Zhang JS, Koenig A, Abel EV, Smyrk TC, Bamlet WR, de Narvajias AA, Gomez TS, Simeone DM, Bujanda L, Billadeau DD: SOX2 promotes dedifferentiation and imparts stem cell-like features to pancreatic cancer cells. *Oncogenesis* 2013;2:e61.
- 35 Wald P, Liu XS, Pettit C, Dillhoff M, Manilchuk A, Schmidt C, Wuthrick E, Chen W, Williams TM: Prognostic value of microRNA expression levels in pancreatic adenocarcinoma: a review of the literature. *Oncotarget* 2017;8:73345-73361.
- 36 Zeng LP, Hu ZM, Li K, Xia K: miR-222 attenuates cisplatin-induced cell death by targeting the PPP2R2A/Akt/mTOR Axis in bladder cancer cells. *J Cell Mol Med* 2016;20:559-567.
- 37 Meng Q, Rayala SK, Gururaj AE, Talukder AH, O'Malley BW, Kumar R: Signaling-dependent and coordinated regulation of transcription, splicing, and translation resides in a single coregulator, PCBP1. *Proc Natl Acad Sci U S A* 2007;104:5866-5871.

- 38 Wei D, Wang L, Kanai M, Jia Z, Le X, Li Q, Wang H, Xie K: KLF4 α up-regulation promotes cell cycle progression and reduces survival time of patients with pancreatic cancer. *Gastroenterology* 2010;139:2135-2145.
- 39 Denicourt C, Saenz CC, Datnow B, Cui XS, Dowdy SF: Relocalized p27Kip1 tumor suppressor functions as a cytoplasmic metastatic oncogene in melanoma. *Cancer Res* 2007;67:9238-9243.
- 40 Costa-Silva B, Aiello NM, Ocean AJ, Singh S, Zhang H, Thakur BK, Becker A, Hoshino A, Mark MT, Molina H, Xiang J, Zhang T, Theilen TM, Garcia-Santos G, Williams C, Ararso Y, Huang Y, Rodrigues G, Shen TL, Labori KJ et al.: Pancreatic cancer exosomes initiate pre-metastatic niche formation in the liver. *Nat Cell Biol* 2015;17:816-826.
- 41 Matsushita H, Yang YM, Pandol SJ, Seki E: Exosome Migration Inhibitory Factor as a Marker and Therapeutic Target for Pancreatic Cancer. *Gastroenterology* 2016;150:1033-1035.
- 42 Li J, Yang X, Guan H, Mizokami A, Keller ET, Xu X, Liu X, Tan J, Hu L, Lu Y, Zhang J: Exosome-derived microRNAs contribute to prostate cancer chemoresistance. *Int J Oncol* 2016;49:838-846.
- 43 Ge Q, Zhou Y, Lu J, Bai Y, Xie X, Lu Z: miRNA in plasma exosome is stable under different storage conditions. *Molecules* 2014;19:1568-1575.